Universiteit Leiden
The Netherlands

Characterisation of uniformly C-13, N-15 labelled bacteriochlorophyll a and bacteriopheophytin a in solution and in solid state: complete assignment of the C-13, H-1 and N-15 chemical shifts

Egorova-Zachernyuk, T.A.; Rossum, B.J. van; Erkelens, C.; Groot, H.J.M. de

Citation
Egorova-Zachernyuk, T. A., Rossum, B. J. van, Erkelens, C., & Groot, H. J. M. de. (2008). Characterisation of uniformly C-13, N-15 labelled bacteriochlorophyll a and bacteriopheophytin a in solution and in solid state: complete assignment of the C-13, H-1 and N-15 chemical shifts. *Magnetic Resonance In Chemistry*, *46*(11), 1074-1083. doi:10.1002/mrc.2295

Version:	Publisher's Version
License:	Licensed under Article 25fa Copyright Act/Law (Amendment Taverne)
Downloaded from:	https://hdl.handle.net/1887/3455019

Note: To cite this publication please use the final published version (if applicable).

Magnetic Resonance in Chemistry

Received: 9 April 2008 Revised: 29 June 2008 Accepted: 2 July 2008 Published online in Wiley Interscience: 19 September 2008

(www.interscience.com) DOI 10.1002/mrc.2295

Characterisation of uniformly ^{13}C, ^{15}N labelled bacteriochlorophyll *a* and bacteriopheophytin *a* in solution and in solid state: complete assignment of the ^{13}C, ^{1}H and ^{15}N chemical shifts

Tatiana Egorova-Zachernyuk,[a,b]* Barth van Rossum,[a†] Cees Erkelens[a] and Huub de Groot[a]

In this investigation we report a complete assignment of ^{13}C, ^{1}H and ^{15}N solution and solid state chemical shifts of two bacterial photosynthetic pigments, bacteriochlorophyll (BChl) *a* and bacteriopheophytin (BPheo) *a*. Uniform stable-isotope labelling strategies were developed and applied to biosynthetic preparation of photosynthetic pigments, namely uniformly ^{13}C, ^{15}N labelled BChl *a* and BPheo *a*. Uniform stable-isotope labelling with ^{13}C, ^{15}N allowed performing the assignment of the ^{13}C, ^{15}N and ^{1}H resonances. The photosynthetic pigments were isolated from the biomass of photosynthetic bacteria *Rhodopseudomonas palustris* 17001 grown in uniformly ^{13}C (99%) and ^{15}N (98%) enriched medium. Both pigments were characterised by NMR in solution (acetone-d_6) and by MAS NMR in solid state and their NMR resonances were recorded and assigned through standard liquid 2D ^{13}C–^{13}C COSY, ^{1}H–^{13}C HMQC, ^{1}H–^{15}N HMBC and solid 2D ^{13}C–^{13}C RFDR, ^{1}H–^{13}C FSLG HETCOR and ^{1}H–^{15}N HETCOR correlation techniques at 600 MHz and 750 MHz. The characterisation of pigments is of interest from biochemical to pharmaceutical industries, photosynthesis and food research. Copyright © 2008 John Wiley & Sons, Ltd.

Keywords: ^{13}C; ^{1}H; ^{15}N; magic angle spinning NMR; multinuclear magnetic resonance; uniform labelling; stable isotopes; bacteriochlorophyll; bacteriopheophytin; photosynthesis; ligand

Introduction

Bacteriochlorophylls are the main pigment species taking part in the primary processes of photosynthesis in anoxygenic photosynthetic bacteria. The characterisation of pigments is important for fundamental research, for the study ligand–protein interactions[1] and functional diversity,[2] for medical applications of porphyrin derivatives as drugs[3] and for food industry.[4] It demonstrates characterisation of natural products in the context of the growing importance of natural products in new medical technologies, in food and feed ingredients and as biofuels.[5]

The chemical structure of BChl is depicted in Fig. 1(a) The basic structure of bacteriochlorophyll *a* (BChl *a*) is a porphyrin ring that can be distinguished from other porphyrins like haem by the presence of a fifth cyclopentanone ring and a coordinated Mg^{2+} ion. Chlorophylls function both as light-harvesting pigments in the antenna and as primary donors in the reaction centres of photosynthetic systems. Another important pigment in the photosynthetic energy conversion process is bacteriopheophytin (BPheo) *a*, since the primary electron acceptor in photosynthesis can be either BChl *a* or BPheo *a*. It differs from the BChl *a* by lacking a coordinated Mg^{2+} ion and having two protons (Fig. 1(a)). BPheo *a* can be easily obtained under acidic conditions from BChl *a*.

To pave the way for magic angle spinning nuclear magnetic resonance (MAS NMR) studies of the chemical and electronic structures of pigments in membrane protein complexes it is important to characterise pure pigments or cofactors. Some studies on plant pigments have been reported already. Solution assignment and re-assignments of ^{13}C and ^{1}H resonances of the plant pigment chlorophyll have been reported in the past in a number of investigations[6,7] that are summarised in Ref. [8] using samples which were biosynthetically ^{13}C enriched to 90% and 15% levels. The difficulty in enriching the bacteriochlorophylls had restricted previous research in their ^{13}C spectra.[8] A natural abundance ^{13}C NMR spectrum of BChl *a* in solution was reported in Ref. [9], using a mixed-solvent system, methanol–pyridine (1 : 4), in order to stabilise the concentrated solution. The ^{13}C chemical shifts of BChl *a* were only assigned using the magnitude spectrum and the assignment was based partly on the assignment of Chl *a* reported in Ref. [7]. Further corrections of the spectral

* *Correspondence to: Tatiana Egorova-Zachernyuk, Protein Labelling Innovation, BioScience park Archimedesweg 27 2333 CM Leiden, The Netherlands. E-mail: proteinlabelling@zonnet.nl*

a *Leiden Institute of Chemistry, Gorlaeus Laboratories, Leiden University, 2300 RA Leiden, The Netherlands*

b *Lomonosov State Academy of Fine Chemical Technology, 117571 Vernadsky 86, Moscow, Russia*

† *Leibniz-Institut für Molekulare Pharmakologie Robert-Rössle-Str. 10; 13125 Berlin, Germany*

Copyright © 2008 John Wiley & Sons, Ltd.

Magnetic Resonance in Chemistry

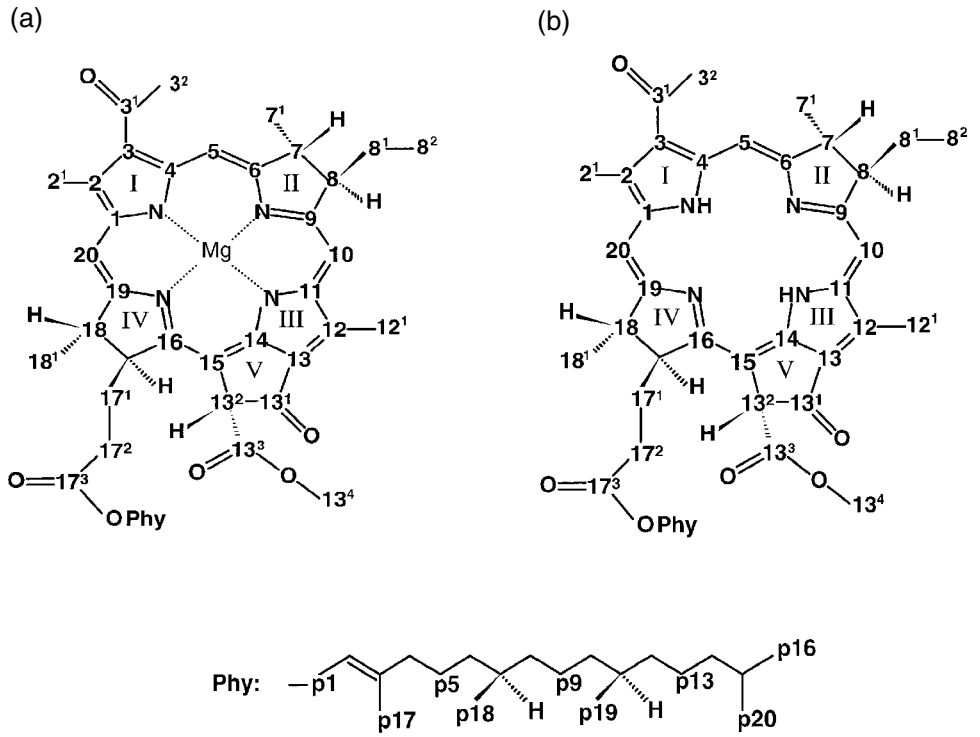

Figure 1. Chemical structures of BChl *a* (a) and BPheo *a* (b) with the International Union of Pure and Applied Chemistry (IUPAC) numbering scheme.

assignment of BChl *a* were described in the literature[10,11] and within the context of study of the pathway of the BChl biosynthesis, selective stable-isotope labelling of BChl *a* of *Rhodopseudomonas spheroides*[10] and of *Chromatium vinosum*[11] was performed in the presence of metabolic precursors such as L-[1-^{13}C] glutamate and [2-^{13}C] glycine. The density functional theory calculations of the structure and ^{15}N and ^{13}C chemical shifts of BChl *a* strongly suggested that several assignments of the ^{13}C resonances of the pyrrolic ring carbons should be revised.[12] The ^{1}H NMR spectrum of BChl *a* was reported in Refs [13–15] and the observed chemical shifts were in agreement with the values reported for acetone but differed markedly from those recorded in pyridine-D_5 solution.[7] The ^{15}N NMR data for BChl *a* in solution were reported in Refs [16,17]. Thus controversial assignments, mis-assignments and re-assignments have been reported for these bacterial pigments either using natural abundance molecules or applying selective stable-isotope labelling.

The extensive role of various isotopic labelling techniques in elucidating the pathway of tetrapyrrole-pigment biosynthesis including the research of David Shemin who introduced isotopic tracer technique is discussed in the literature.[18] Isotopic replacement of pigments and a lipid in chlorosomes and characterisation of the chlorosomes are described in Ref. [19]. Advantages of uniform stable-isotope labelling have been shown earlier; biosynthetic ^{13}C labelling strategies of the plant pigment pheophytin (Phe a) were described by us in Ref. [20] and their application allowed complete ^{13}C assignment of Phe and its study in the photosynthetic membrane protein complex of *Rhodobacter sphaeroides* R-26; uniform biosynthetic ^{13}C, ^{15}N labelling of bacterial Pheo (BPheo *a*) allowed assignment of its modes and discrimination from those of the reaction centre protein of *R. sphaeroides* R-26 using Fourier transform infrared spectroscopy (FTIR)-difference spectroscopy.[21] Finally selective chemical shift assignment of both B800 and B850 has been performed in LH2 of *Rhodopseudomonas acidophila* 10 050.[22]

In this investigation we report a complete assignment of ^{13}C, ^{1}H and ^{15}N solution and solid state chemical shifts of two bacterial photosynthetic pigments, BChl *a* and BPheo *a*. This became possible via applying uniform stable-isotope labelling strategies and isolating both pigments [U–^{13}C, ^{15}N] BChl *a* and [U–^{13}C, ^{15}N] BPheo *a* from the biomass of the photosynthetic bacteria. The isotopic enrichment for both pigments for ^{13}C and ^{15}N nuclei is >99% and 98% respectively.

Results and Discussion

Uniform stable-isotope labelling of biomolecules is a powerful tool for structural studies since it allows performing NMR studies on a single uniformly labelled sample and could be achieved biosynthetically by culturing a chosen micro-organism on a medium containing uniformly ^{13}C, ^{15}N labelled substrates as metabolic precursors. Issues related with cost-effective preparation of uniformly labelled biomass of photosynthetic organisms are discussed in the literature.[23–25] Uniformly ^{13}C, ^{15}N enriched BChl *a* (Fig. 1(a)) was isolated from the biomass of photosynthetic bacteria *Rhodopseudomonas palustris* 17 001 grown on uniformly labelled medium as described in Ref. [21]. Uniformly ^{13}C, ^{15}N enriched BPheo *a* (Fig. 1(b)) was obtained from the ^{13}C, ^{15}N uniformly enriched BChl *a* under acidic conditions.[26] The NMR results from three independent preparations of the pigments that were reproducible.

From the solution and solid state NMR data collected with the homonuclear (^{13}C–^{13}C) correlation technique the assignment of the carbon resonances was first obtained. The carbon assignment was used to assign the proton chemical shifts in 2D (^{1}H–^{13}C) heteronuclear correlation spectra. Since ^{13}C shifts are generally

 Copyright © 2008 John Wiley & Sons, Ltd.

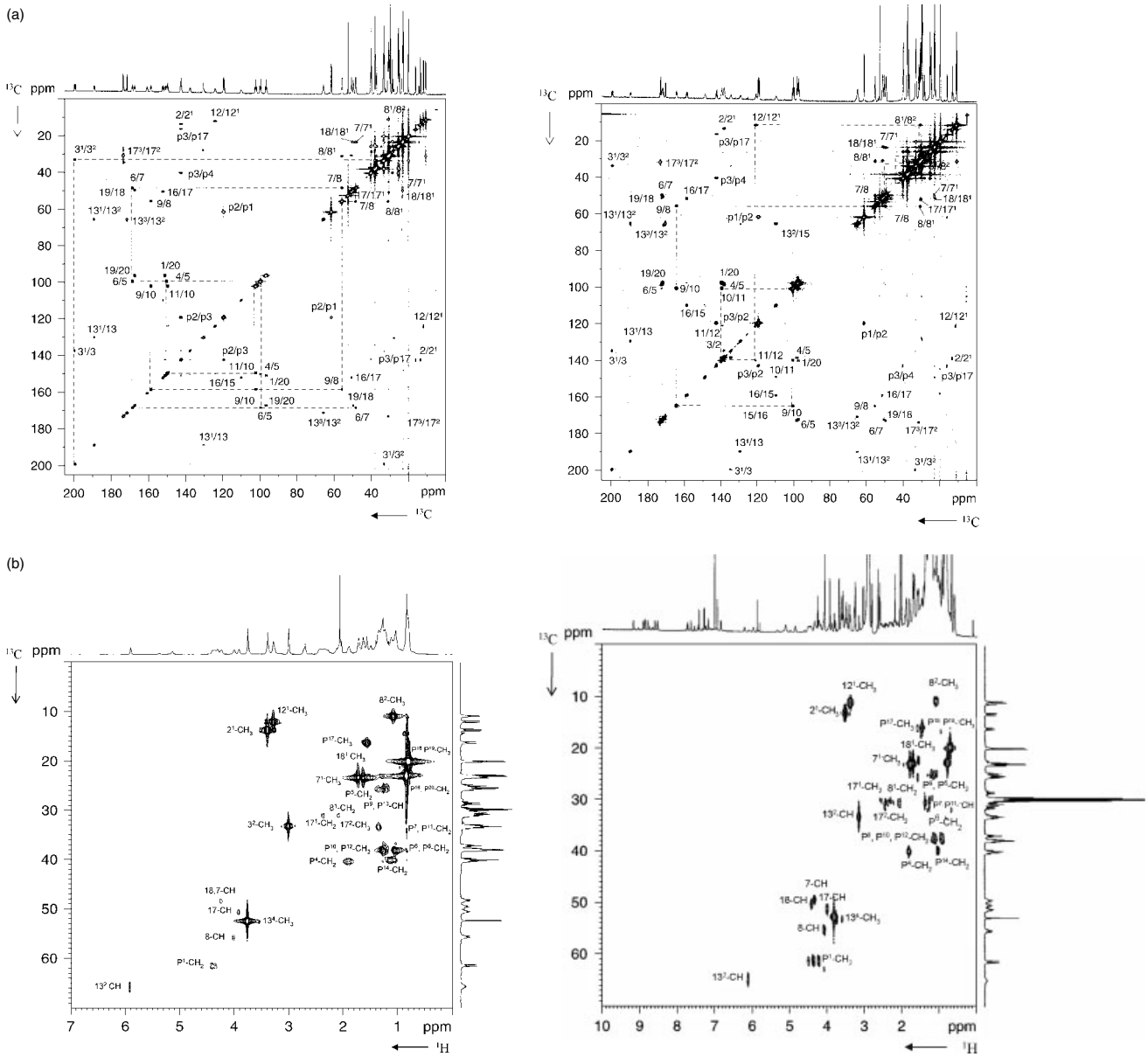

Figure 2. Contour plot of a 2D $^{13}C-^{13}C$ COSY (a), 2D $^{1}H-^{13}C$ HMQC (b) and $^{1}H-^{15}N$ HMBC (C) NMR dipolar correlation spectra of [U–^{13}C, ^{15}N] BChl *a* in acetone-d_6 (left panel) and of [U–^{13}C, ^{15}N] BPheo *a* in acetone-d_6 (right panel) recorded in a magnetic field of 14.1 T at room temperature. The assignments of correlations (*x*/*y*) on the plot correspond with the numbering of pigments in Fig. 1.

quite sensitive to atomic charge density variations, the shifts provided information about the electronic structure of the molecule at the atomic level. The proton assignment was used to assign nitrogen chemical shifts in 2D ($^{15}N-^{1}H$) heteronuclear correlation spectra. Characterisation of U–^{13}C, ^{15}N BChl *a* and of U–^{13}C, ^{15}N BPheo *a* in solution is presented in Fig. 2 and in solid state in Figs 3 and 4 on the left and right panels respectively. Figure 5 shows ^{13}C and ^{1}H chemical shift correlation plots of BChl *a* and BPheo *a*.

The 2D homonuclear $^{13}C-^{13}C$ correlation spectrum of the [U–^{13}C, ^{15}N] BChl *a* in solution is presented in Fig. 2(a) (left panel). From the high-field 2D $^{13}C-^{13}C$ homonuclear correlation spectrum of [U–^{13}C, ^{15}N] BChl *a*, the following nearest-neighbour $^{13}C-^{13}C$ correlation networks in the molecule of [U–^{13}C, ^{15}N] BChl *a* are clearly seen: C4-C5-C6-C7-C8-C9-C10-C11-C-12; C13-$C13^1$-$C13^2$; C15-C16-C17-C18-C19-C20-C1-C2. In addition there are correlations between C3–$C3^1$–$C3^2$, C7–$C7^1$, C8–$C8^1$–$C8^2$, C12–$C12^1$, $C13^2$–$C13^3$ and C17–$C17^1$–$C17^2$–$C17^3$.

Although no correlations are observed between C2–C3, C3–C4, C12–C13, C13–C14, C14–C15 and $C13^2$–C15, these signals are clearly present on the diagonal and the correlations with the other neighbouring atoms are clearly seen. For example, C2 has been assigned from C2–$C2^1$, C3 from C3–$C3^1$, C4 from C4–C5, C12 from C12–C11 and C12–$C12^1$, C13 from C13–$C13^1$, and C15 from C15–C16. Finally the C14 corresponds to the data from the literature.[10]

In the phytyl chain there are the correlations between p1-p2-p3-p4-p5-p6-p7-p8-p9-p10. There are also the correlations observed between p3 and p17, p7 and p18, p11 and p19, and p16 and

Copyright © 2008 John Wiley & Sons, Ltd.

Magnetic Resonance in Chemistry

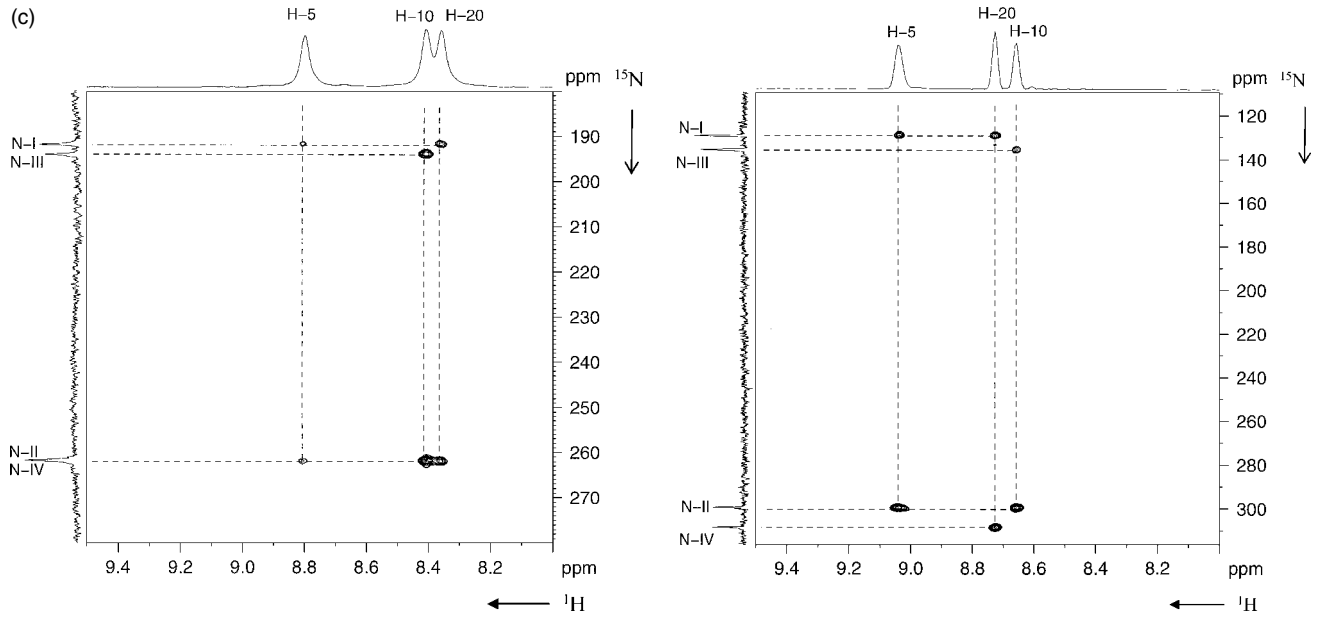

Figure 2. (*Continued*).

p20. Definite assignments were found for $C8^1$, $C13^2$, $C17^1$, $C17^2$ and C19.

The 2D homonuclear $^{13}C-^{13}C$ correlation spectrum of the [U–^{13}C, ^{15}N] BPheo *a* in solution is presented in Fig. 2(a) (right panel). Following nearest-neighbour $^{13}C-^{13}C$ correlation networks in the molecule of [U–^{13}C, ^{15}N] BPheo *a* are clearly seen: C13-C14-C15-C16-C17-C18-C19-C20-C1-C2-C3-C4-C5-C6-C7-C8-C9-C10-C11-C12. In addition there are correlations between $C3-C3^1-C3^2$ in the ring I, $C7-C7^1$ and $C8-C8^1-C8^2$ in the ring II, $C12-C12^1$ in the ring III, $C17-C17^1$ and $C17^2-C17^3$ in the ring IV, and $C13^2-C13^3$ in the ring V. In the phytyl chain there are the correlations between p1-p2-p3-p4-p5-p6- p7-p8-p9-p10. There are also the correlations between p3 and p17, p7 and p18, p11 and p19, and p16 and p20. Several chemical shifts values are less resolved, namely for C1 and C11, $C17^1$ and $C17^2$ and finally p18, p19 and p20.

The 2D homonuclear $^{13}C-^{13}C$ dipolar correlation MAS NMR data collected from the [U–^{13}C, ^{15}N] BChl *a* recorded with the radio frequency–driven dipolar recoupling (RFDR) technique are presented in Fig. 3(a) (left panel). MAS sideband diagonals at $\omega_r/2\pi = 9000 \pm 5$ Hz are clearly visible, as well as strong 2D cross-peaks revealing the transfer of coherence. Several of the cross-peaks and diagonal peaks are connected by lines, illustrating how they contribute to a correlation network revealing the molecular framework, similar to the assignment procedures in solution NMR. The high-spinning frequency used for the experiment in Fig. 3 (a) minimises the occurrence of rotational resonance effects and of overlap between the correlated peaks and sideband lines. The lines in Fig. 3(a) connecting cross-peaks and diagonal peaks illustrate how the molecular ^{13}C framework gives rise to a correlation network. The data were acquired in a high static magnetic field, using a high-spinning frequency and the efficient two pulse phase modulation (TPPM) proton decoupling technique.[27]

For a short mixing time, ~1 ms, the correlations in the MAS NMR are predominantly associated with nearest-neighbour carbon–carbon connectivities. Assignment of BChl *a* resonances was based on a detailed analysis of the two spectra collected with spinning frequency of 9000 and 13 000 Hz. The assignment procedure of [U–^{13}C, ^{15}N] BChl *a* led to the identification of several extended nearest-neighbour solid state ^{13}C correlation networks in the molecule such as C1-C2-C3-C4-C5-C6-C7-C8-C9-C10-C11-C12-C13, C14-C15-C16-C17 and C18-C19-C20-C1. In addition there are the correlations $C3-C3^1-C3^2$, $C12-C12^1$, $C13-C13^1-C13^2-C13^3$, and $C2-C2^1$. In the phytyl chain of BChl *a* there is the correlation between p1-p2-p3-p4-p5-p6-p7-p8. Finally, there is a correlation between p3 and p17. Doubling of peaks is observed for p3–p4 and p3–p17. Some of these correlation networks, involving the strongest cross-peaks, are depicted in Fig. 3(a) with the dashed lines. Although all peaks are present on a diagonal there are no strong correlations between C7–C8, $C8-C8^1$, $C7-C7^1$, $C18-C18^1$, $C17-C17^1$ and $C17^1-C17^2$.

Characterisation of [U–^{13}C, ^{15}N] BPheo *a* has been performed as described above for [U–^{13}C, ^{15}N] BChl *a*. From the Fig. 3(a) right panel the assignment procedure led to the identification of the following nearest-neighbour ^{13}C correlation networks in the molecule of [U–^{13}C, ^{15}N] BPheo *a*: C3-C4-C5-C6-C7; C8-C9-C10-C11-C12-C13-C14-C15-C16-C17-C18-C19-C20-C1-C2-C3. In addition there are correlations $C2-C2^1$ and $C3-C3^1-C3^2$ in the ring I, $C8-C8^1$ in the ring II, $C12-C12^1$ in the ring III, $C17^2-C17^3$ in the ring IV, and $C13^2-C13^3$ in the ring V.

Although no correlations are observed between $C7-C7^1$, $C8-C8^1$, $C17-C17^1$ and $C18/C18^1$, these signals are clearly seen on the diagonal. Some of these correlation networks are depicted in Fig. 3(a) with the dashed lines. It should be mentioned that C4–C5 and C10–C11, C3–C4 and C12–C13 are strongly overlapping and the chemical shifts of C1, C4, C11, and C2 are very similar; the shifts for $C3^2$, $C8^1$, $C17^1$ and $C17^2$ are also very similar.

In the phytyl chain of BPheo *a* the following correlation network is observed: p1-p2-p3-p4-p5-p6-p7-p8-p9. Finally, there is a very clear correlation between p3 and p17. There is overlap observed for p8-p6-p10-p12, p7-p11, p5-p9-p13 and p19-p20.

In Table 1 ^{1}H chemical shifts of [U–^{13}C–^{15}N] BChl *a* and [U–^{13}C–^{15}N] BPheo *a* in solution and in the solid state are summarised. The proton assignment for BChl *a* in solution is in agreement with the assignment published earlier with the exception for the protons of $C13^2$ (difference is 1.59 ppm) (see

 Copyright © 2008 John Wiley & Sons, Ltd.

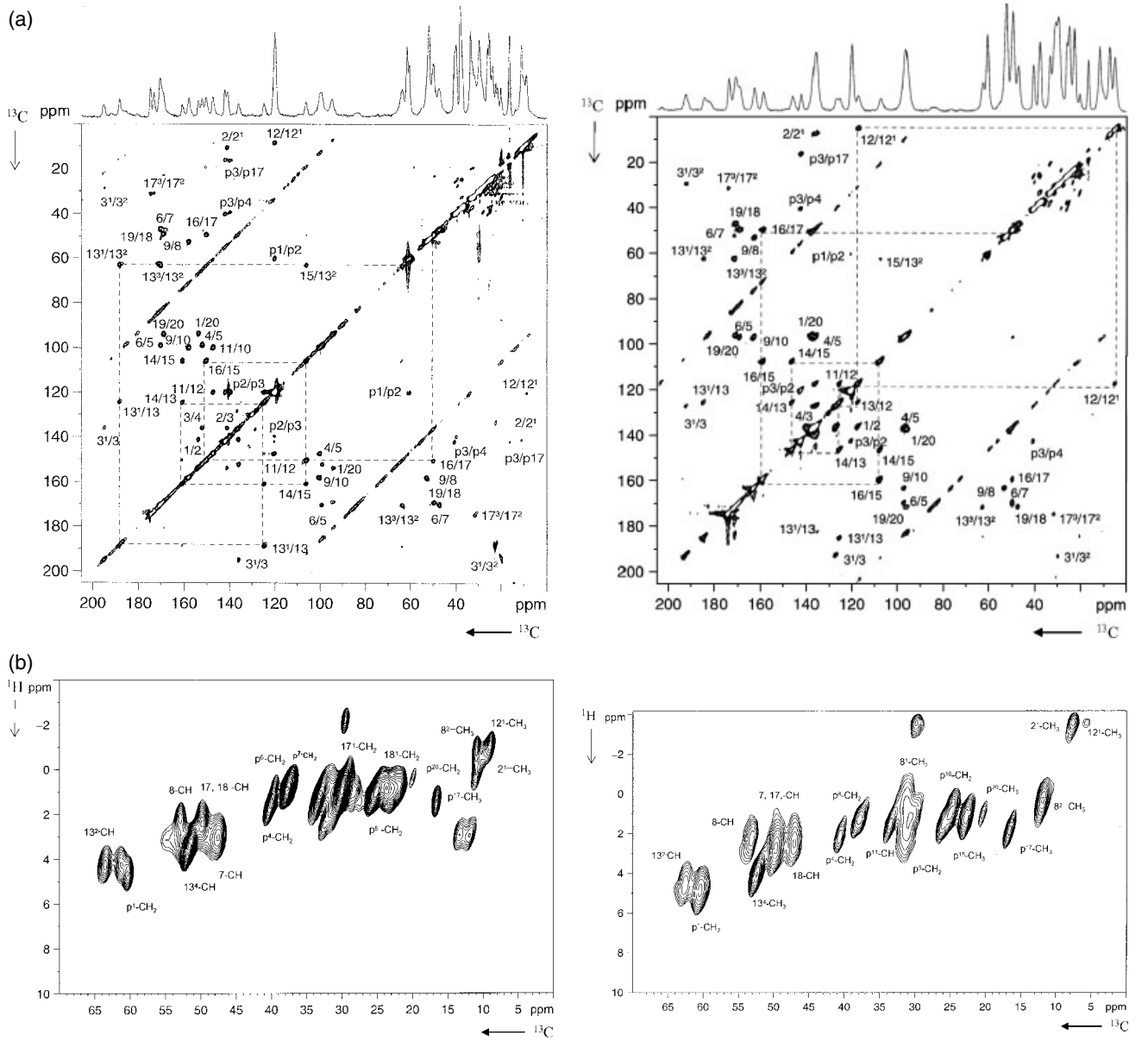

Figure 3. Contour plot of a 2D ^{13}C–^{13}C RFDR MAS NMR (a) and 2D ^{1}H–^{13}C FSLG MAS NMR (b) dipolar correlation spectrum of [U–^{13}C, ^{15}N] BChl *a* (left panel) and of [U–^{13}C, ^{15}N] BPheo *a* (right panel) recorded in a magnetic field of 14.1 T at room temperature. The spinning frequency was 9000 ± 3 Hz for (A) and 13 000 Hz for (b) and the data were collected with a polarisation transfer time of 1 ms. The lines indicate sequences of nearest-neighbour correlations. The assignments of correlations (*x*/*y*) on the plot correspond with the numbering of pigments in Fig. 1.

Table 1). A good resolution can be obtained by ^{13}C detection and by exploiting the large ^{13}C chemical shift dispersion in heteronuclear (^{1}H–^{13}C) correlation spectroscopy. For fast MAS heteronuclear (^{1}H–^{13}C) correlation spectroscopy, the resolution on the proton side can be improved dramatically through the application of frequency-switched Lee–Goldburg (FSLG) irradiation during proton evolution.[28]

In Fig. 3(b) we present a high-field and high-spinning speed 2D ^{13}C–^{1}H heteronuclear FSLG decoupled correlation data collected from [U–^{13}C] BChl *a* and [U–^{13}C] BPheo *a*. The data were recorded using a modified version of the pulse sequence discussed in Ref. [28]. The assignment of the proton chemical shifts was performed after the assignment for carbon was completed. The proton–carbon correlations are well resolved, also in the aliphatic region of the spectrum. The overall sensitivity is good, owing to the high-spinning frequency used for the experiment. The proton lines are also partially resolved in the F1 projection, which underlines the good overall performance of the FSLG decoupling.

On the basis of proton chemical shifts assignments obtained in solution and in solids, ^{15}N chemical shifts of [U–^{13}C, ^{15}N] BChl *a* and [U–^{13}C, ^{15}N] BPheo *a* were assigned and are summarised in Table 2 (see also Figs 2(c), 3(b) and 4).

Uniformly labelled samples allow complete assignment of all resonances and in Table 3 the chemical shifts for the BChl *a* in acetone-d_6 are compared with the chemical shifts published earlier in acetone-d_6 methanol-d_4 (4 : 1).[10] For several atoms very different assignments have been found, compared with the

Copyright © 2008 John Wiley & Sons, Ltd.

Magnetic Resonance in Chemistry

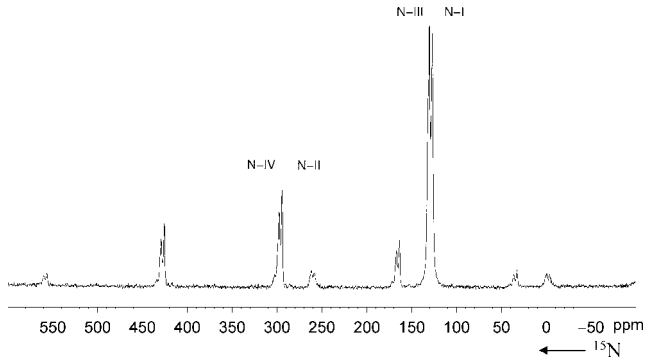

Figure 4. The ^{15}N MASNMR spectrum of [U–^{13}C–^{15}N] BPheo *a*. The spinning frequency was 8000 Hz.

assignments published in Ref. [10]; the comparisons are as follows for the C2, C3 in ring I, C6, C9 in ring II, C12, C13 in ring III, C16 in ring IV: C2 (142.0 vs 127.6), C3 (137.7 vs 122.3); C6 (168.9 vs 140.6), C9 (158.5 vs 151.7); C12 (124.0 vs 135.1), C13 (130.6 vs 156.6); C16 (152.0 vs 160.2). C13 and C3^2 were assigned in this work. This demonstrates the utility of the uniform labelling strategies for NMR applications.

For the other ^{13}C responses listed in Table 3, the shift variations due to effects associated with the two different solvents are less than 2.5 ppm. Our assignment of C5, C10, C15, C20, C4 and C14 is in agreement with the corrected assignments for the carbons published in Ref. [12].

The ^{1}H and ^{13}C shifts in the solid and solution samples are plotted against monomer shifts in acetone-*d6* in Fig. 5(a,b) respectively. When ^{13}C solid state chemical shifts are compared with solution chemical shifts for [^{13}C–^{15}N] BChl *a* obtained in this work, the largest differences are observed for C2^1 (−2.6), C3^1 (−4.7), C3^2 (−2.9), C12^1 (−3.2), C13^4 (−2.3); C13 (−6.5), C15 (−3.9), C8 (−3.6), C10 (−2.7) and C20 (−2.4), which are upfield shifted by 3–5 ppm while downfield shifts are detected for C1 (2.3), and C17^2 (3.1) by about 2–3 ppm (see Fig. 5(a). When the ^{1}H solid state chemical shifts are compared with the solution data, large differences are seen for C2^1–CH$_3$ and C12^1–CH$_3$ providing evidence for ring current shifts due to aggregation in the solid state.

By comparison of solid state chemical shifts with solution chemical shifts for [U–^{13}C–^{15}N] BPheo *a* (Table 4), the biggest differences are observed for C1 (−2.8 ppm), C2^1 (−6.6 ppm), C3 (7.9 ppm), C3^1 (−7.0 ppm), C3^2 (−4.7); C6 (−3.5); C10 (−3.5 ppm), C11 (−3.4), C12 (−4 ppm), C12^1 (−6.6 ppm); C13^1 (−4.5), C13^2 (−3.1), C14 (−2.8) and C18 (−3.3 ppm) which are upfield shifted by 3–7 ppm.

For the carbon assignment for [U–^{13}C–^{15}N] BPheo *a versus* [U–^{13}C–^{15}N] BChl *a* in solution the largest differences are found in ring I for C1 (−13.6 ppm), C2 (−6.1 ppm), C3 (−10.6 ppm) and C4 (−14.1 ppm); in ring II for C9 (12.6 ppm); in ring III for C11 (−13.6 ppm) and C14 (−14.9 ppm) and in ring IV for C16 (6.7 ppm) and C19 (3.8 ppm).

For the solid state carbon assignment of the two pigments, the following differences in the values of chemical shifts are observed: in ring I for C1 (−16.6 ppm), C2 (−5 ppm), C2^1 (−3.6 ppm), C3 (−8.6 ppm) and C4 (−16.0 ppm); in ring II for C9 (4.7 ppm); in ring III for C11 (−11.2 ppm) and for C14 (−14.7 ppm); in ring IV for C16 (−9 ppm); in ring V for C^{13} (−3.6 ppm). For methine carbons, the differences are C10 (−3.0 ppm), C5 (−2.4 ppm) and C20 (−2.2 ppm). The result implies that the structure and electronic states are significantly influenced by the presence of the central magnesium ion in the molecule of BChl *a*.

Table 1. Assignment of ^{1}H chemical shifts of [U–^{13}C–^{15}N] BChl *a* and [U–^{13}C–^{15}N] BPheo *a*. Assignments of chemical shifts in tetrahydrofurane (THF), $\delta*$ (ppm) are presented as described in Ref. [14]. Assignments of chemical shifts in acetone-d_6, δ (ppm), and solid state chemical shifts, δ_c (ppm), are obtained on a uniformly labelled sample (this work). The accuracy of the solid state shifts is ~0.2 ppm

Position	BChl *a* $\delta*$	BChl *a* δ	BChl *a* δ_c	BPheo *a* δ	BPheo *a* δ_c
5	9.00	8.81	6.75	9.05	7.04
10	8.46	8.40	5.50	8.66	5.10
20	8.36	8.36	5.89	8.73	5.80
13^2	4.33	5.92	4.31	6.10	4.59
7	4.09	4.24	3.06	4.35	2.73
17	4.01	3.92	2.45	3.99	2.73
18	4.35	4.32	2.45	4.41	2.45
8	nd	4.03	2.17	4.07	2.22
8^1	2.37/2.12	2.08	0.96	2.07	1.2
2^1	3.46	3.40	−0.84	3.5	nd
3^2	3.03	3.01	0.96	2.07	1.18
7^1	nd	1.73	0.85	1.8	0.85
8^2	1.15	1.09	−0.78	1.09	0.34
12^1	3.38	3.29	−1.02	3.20	nd
18^1	1.68	1.65	0.86	1.70	nd
13^4	3.71	3.76	3.46	3.76	4.07
17^1	2.53	2.37	0.96	2.4	nd
17$^{1'}$	2.33	2.45	nd	nd	nd
17^2	2.42	2.45	0.96	2.30	nd
17$^{2'}$	2.13	2.04	nd	nd	nd
p1	4.51	4.39	4.26	4.26	4.84
p2	5.24	5.13	5.45	5.20	5.80
p17	1.63	1.58	1.44	1.50	1.83
p4	1.95	1.91	1.49; 1.67	1.93	2.15
p5	1.43	1.35	1.02	1.45	1.18
p15	nd	1.17; 1.04	0.96	1.25	1.18
p6	1.04	1.09	0.79	1.17; 1.04	1.27
p8	nd	1.09	1.49	1.09	1.27
p10	nd	1.13	1.49	1.09	1.27
p12	nd	1.13	1.49	1.09	1.27
p14	nd	1.11	1.49	1.04	1.27
p7	0.88	0.89	1.07	1.35; 1,26	1.56
p11	0.86	0.89	0.96	1.28	1.56
p9	0.84	1.28	1.02	1.21	1.18
p13	nd	1.21	1.02	1.21	1.18
p16	nd	0.84	0.86	0.84	1.14
p18	nd	0.81	0.40	0.82	1.06
p19	nd	0.81	0.40	0.82	1.06
p20	nd	0.83	0.40	0.92	1.14

nd, not determined.

Experimental

Sample preparation

To obtain uniformly enriched pigments, photosynthetic bacteria *R. palustris* 17 001 were grown on a medium containing:

 Copyright © 2008 John Wiley & Sons, Ltd.

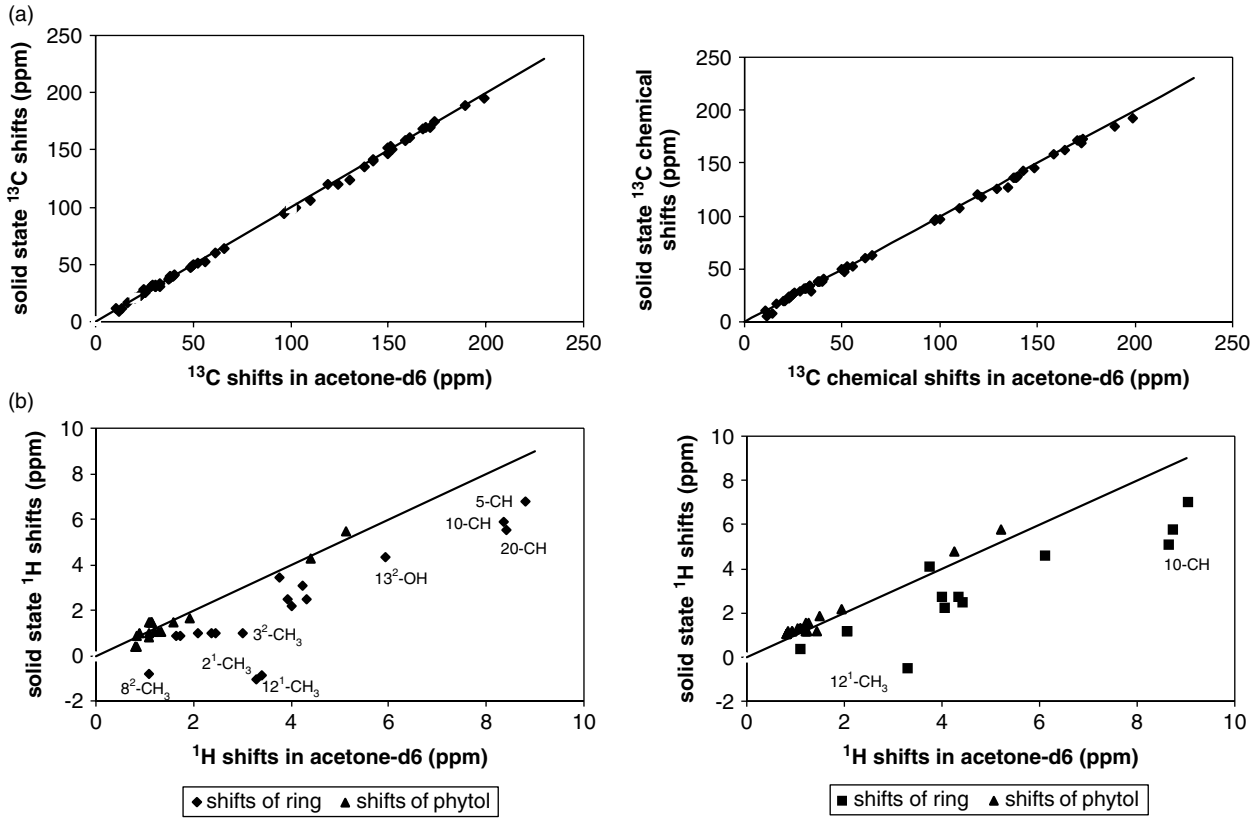

Figure 5. ^{13}C and ^{1}H chemical shift correlation plots of [U–^{13}C, ^{15}N] BChl *a* (left panel) and of [U–^{13}C, ^{15}N] BPheo *a* (right panel). The ^{1}H and ^{13}C shifts in the solid sample are plotted against the monomer shifts in acetone-d_6 solution. The solid lines represent the diagonals. Several ^{1}H signals are indicated that show a large up field shift in the solid compared with the monomer.

Table 2. ^{15}N chemical shift of [U–^{13}C–^{15}N] BChl *a* and [U–^{13}C–^{15}N] BPheo *a*. $\delta*$ (ppm) – values of nitrogen chemical shift in acetone as published in Ref. [16], δ (ppm) solution chemical shift (this work); δ_c (ppm) – solid state chemical shift (this work)

Position	BChl *a* $\delta*$	BChl *a* δ	BChl *a* δ_c	BPheo *a* δ	BPheo *a* δ_c
N-I	189.6	192.63	191.76	129.4	127.2
N-III	191.5	194.46	196.87	135.7	132.5
N-II	258.5	259.14	258.28	299.2	296.07
N-IV	259.1	261.71	258.28	308.3	303.17

[U–^{13}C, ^{15}N] algae hydrolysate (Heidelberg, EMBL) – 2.5 g l^{-1}, KH_2PO_4 (Darmstadt, Germany) – 1 g l^{-1}, $MgSO_4 \times 7H_2O$ (Darmstadt, Germany – 0.4 g l^{-1}, NaCl (Darmstadt, Germany) – 0.4 g l^{-1}, $CaCl_2 \times 2H_2O$ (Darmstadt, Germany) – 0.05 g l^{-1}, and trace metals – 10 ml l^{-1}. NaOH (1 N) was used for the adjustment to pH 7. The solution of trace elements was prepared as described for M 550 in Ref. [21], but $Na_2MoO_4 \times 2H_2O$ was used instead of $(NH_4)_6 Mo_7O_{24} \times 4H_2O$ and ethylenediaminetetraacetic acid (EDTA) was excluded. The light intensity was 2 klux obtained from incandescent lamps.

After 20 days of growing, the cells were harvested by centrifugation (15 min at 10 000 *g*) and the pigments were extracted by incubating under mild sonication (Standardgraph, Ultrasonic cleaner) at 4 °C for 2 min in a 20-fold volume of acetone and centrifuged at 5400 *g* for 10 min. The supernatant consisted mostly of carotenoid pigments. The precipitate was extracted with MeOH and centrifuged at 5400 *g* for 20 min, releasing the BChls in the supernatant. The acetone and methanol extracts were filtered over a 0.45 μm teflon (TOSOH H-25-5) membrane filter separately, dried at reduced pressure with a rotary evaporator and subsequently dissolved in a mixture of *n*-hexane, 2-propanol, and methanol

Table 3. Assignment of ^{13}C chemical shifts of [U–^{13}C–^{15}N] BChl *a* in solution and in solid state). Assignments of chemical shifts: $\delta*$ (ppm) – in acetone-d_6–methanol-d_4, as described earlier in Ref. [9] and further corrected in Ref. [10]; δ (ppm) – in acetone-d_6 and δ_c (ppm) in solid state, both obtained in this work based on a uniformly ^{13}C–^{15}N labelled sample. The accuracy of the solid state shifts is ~0.5 ppm. The numbering is according to the chemical structure in Fig. 1(a)

Position	$\delta*$	δ	δ_c	$\Delta = (\delta_c - \delta)$
8^2	9.1	10.5	11.0	0.5
12^1	10.3	11.9	8.7	−3.2
2^1	12.0	13.5	10.9	−2.6
p17	14.1	16.1	16.3; 16.7	0.2; 0.6
p18	21.2; 18.3[a]	20.5	20.5	0.0
p19		20.1; 19.8	20.0	−0.1; 0.2
p20		20.0	20.0	0.0
p16		22.9	23.0	0.1
18^1	21.2	22.8	23.0	0.2
3^2		32.9	30.0	
7^1	21.2	23.4	23.0	−0.4

Copyright © 2008 John Wiley & Sons, Ltd.

Table 3. (*Continued*)

Position	$\delta*$	δ	δ_c	$\Delta = (\delta_c - \delta)$
p5	23.8	25.3	25.0	−0.3
p9	23.6	24.9	27.5	2.6
p13	23.2	25.5	25.0	−0.5
17^2	31–27	29.4	32.5	3.1
17^1	31–27	30.5	30.5	0.0
8^1	31–27	30.8	30.0	−0.8
p7	31.6, 31.4, 31.1[a]	33.3	33.5	0.2
p11		31.0	31.5	0.5
p15		28.6	31.0	1.4
p4	38.2, 38.5[a]	40.2	39.4; 40.2	−0.8
p6		37.6	37.5	−0.5
p8		38.5	39.0	0.5
p10	36.2, 35.3	38.0	38.0	0
p12		37.8	38.0	0.2
p14		39.8	39.0	−0.8
7	46.7	48.3	47.3	−1.0
18	48.0	49.5	49.1	−0.4
17	49.0	50.5	49.6	−0.9
13^4	50.8	52.3	51.5	−0.8
8	54.0	55.8	52.9	−2.9
p1	59.8	61.7	60.3	−1.4
13^2	65.0	65.7	63.3	−2.4
20	94.2 (95.6[b])	96.3	93.9	−2.4
5	97.6 (99.0[b])	99.9	98.9	−1
10	99.9 (101.6[b])	102.4	99.7	−2.7
15	107.1 (109.4[b])	109.7	105.8	−3.9
p2	117.2	119.3	119.9	0.6
2	127.6	142.0	140.9	−1.1
12	135.1	124.0	120.0	−4.0
13		130.6	124.1	−6.5
3	122.3	137.7	135.7	−2.0
p3	141.2	142.4	139.6; 141.9	−2.8; −0.5
11	147.9	149.5	147.1	−2.4
4	147.9 (149.7[b])	150.0	151.9	1.9
1	150.2	151.2	153.5	2.3
16	166.1[a] (160.2[b])	152.0	150.2	−1.8
14	143.8 (158.1[b])	160.8	160.6	−0.2
9	140.6 (151.7[b])	158.5	157.7	−0.8
19	164.9[a]	167.3	168.8	1.5
6	140.6	168.9	170.0	1.1
13^3	170.7	171.6	169.9	−1.7
17^3	171.7	173.4	174.5	1.1
13^1	187.5	189.0	188.4	−0.6
3^1	197.6	199.3	194.6	−4.7

Note: For the solid state correlations C7–$C7^1$ and C17–$C17^1$ are not observed and p3–p4 and p3–p17 appeared as double peaks in the MAS NMR spectra.
[a] Unknown.[9]
[b] Corrected assignment in Ref. [10]

(100/3/3 v/v/v) used as an eluent for high performance liquid chromatography (HPLC). The pigments were separated on a normal phase silica HPLC column (Senshupak, 1251-N, 250 × 4.6 mm i.d.), cooled to 4 °C, using a mixture of *n*-hexane, 2-propanol and methanol (100/3/3 v/v/v) as an eluent. For at least 99% of the BChl in *R. palustris,* phytyl was found to be the esterifying alcohol. The [U–^{13}C, ^{15}N] BPheo *a* fraction was collected and an additional amount of [U–^{13}C, ^{15}N] BPheo *a* was obtained by pheophytinisation of [U–^{13}C, ^{15}N] BChl *a* by bubbling a stream of nitrogen gas containing gaseous HCl into the ether solution of [U–^{13}C, ^{15}N] BChl *a* as described in Ref. [26]. More than 80 mg of stable-isotope-labelled pigments were isolated and used for various applications such as development of pulse sequences for MAS NMR, or fundamental research, in particular, characterisation of pigments and

Table 4. Assignment of ^{13}C-NMR chemical shifts of [U–^{13}C–^{15}N] BPheo *a* in solution and in solid state. Assignments of chemical shifts: δ (ppm) – in acetone-d_6 and δ_c (ppm) – in solid state, are obtained in this work on a uniformly ^{13}C, ^{15}N labelled sample. The accuracy of the solid state shifts is ∼0.5 ppm. The numbering is according to the chemical structure in Fig. 1(b)

Position	δ	δ_c	$\Delta = (\delta_c - \delta)$
2^1	13.9	7.3	−6.6
8^2	11.5	11.0	−0.5
12^1	11.5	4.9	−6.6
p17	16.3	16.5	0.2
p16	22.8	22.0	−0.8
p18	20.5	21.5	1
p19	19.8; 20.0	20.0	0.2; 0
p20	20.0	20.0	0
18^1	22.9	nd	
7^1	23.7	nd	
17^1	31.3	31.0	−0.3
17^2	31.5	31.5	0
8^1	30.7	31.0	0.3
p5	25.3	27.0	1.7
p9	24.9	26.5	1.6
p13	25.0	26.5	1.5
p7	33.2	34.5	1.3
p11	33.2	34.0	0.8
p15	28.6	29.0	0.4
p4	40.2	41.0	0.8
p6	37.6	38.0	0.4
p8	37.9	38.5	0.6
p10	38.5	38.0	−0.5
p12	38.5	38.0	−0.5
p14	39.8	38.0	−1.8
3^2	34.0	29.3	−4.7
7	49.6	49.5	−0.1
18	50.9	47.6	−3.3
17	51.4	49.5	−1.9
13^4	52.8	52.5	−0.3
8	55.4	53.0	−2.4
p1	61.7	60.3	−1.4
13^2	65.5	62.4	−3.1
20	97.2	96.1	−1.1
5	97.9	96.5	−1.4
10	100.2	96.7	−3.5
15	110.3	107.9	−2.4
p2	119.4	120.3	0.9
2	138.5	135.9	−2.6
13	129.2	125.5	−3.7
3	135.0	127.1	−7.9
12	121.3	117.3	−4.0
4	138.1	135.9	−2.2
11	139.3	135.9	−3.4

Copyright © 2008 John Wiley & Sons, Ltd.

Table 4. (*Continued*)

Position	δ	δ_c	$8 = (\delta_c - \delta)$
1	139.7	136.9	−2.8
p3	143.0	142.1	−0.9
16	158.7	158.7	0.0
14	148.7	145.9	−2.8
9	164.3	162.4	−1.9
19	171.7	171.1	−0.6
6	172.4	168.9	−3.5
13^3	170.2	171.1	−0.9
17^3	173.0	173.4	0.4
13^1	189.3	184.8	−4.5
3^1	199.2	192.2	−7.0

Note: For solid state the correlations C7-C-7^1, C17-C-17^1 and C18–$C18^1$ are not observed. The values of chemical shifts of (C1, C4, C11, C2) and ($C3^2$, $C8^1$, $C17^1$, $C17^2$) are very similar to each other. In the phytyl chain the following chemical shifts have similar values: p5, p9, p13; p6, p8, p10; p7, p11 and p19, p20.
nd, not determined.

study of ligand–protein interactions as well as for other studies. Both pigments, [U–^{13}C, ^{15}N] BChl *a* and [U–^{13}C, ^{15}N] BPheo *a*, were characterised by optical, NMR and FTIR spectroscopy.

For the solution and CP/MAS NMR experiments, a Bruker 600 MHz DMX spectrometer was used. Solid state MAS NMR experiments were performed on DMX-600 and DSX-750 spectrometers equipped with a double resonance 4 mm CP/MAS probe (Bruker, Karlsruhe, Germany).

For the solution NMR measurements, 3 mg of micro (nano)–crystalline precipitates of [U–^{13}C, ^{15}N] BChl *a* or [U–^{13}C, ^{15}N] BPheo *a* was dissolved in 0.7 ml $^2H_6$-DMSO-acetone and placed in a 5-mm NMR tube, followed by the degassing of the solution with nitrogen gas. For MAS NMR measurements two samples of micro(nano)–crystalline precipitates were measured. They were prepared by placing a solution of the pigment in a 4 mm CRAMPS rotor (Bruker) and evaporating the solvent with nitrogen gas. The sample volume was restricted to the centre of the rotor to improve the RF homogeneity. In a similar way a sample of [U–^{13}C, ^{15}N] BPheo *a* was prepared. For MAS NMR studies an amount of 10 mg of each of the pigments was used. Solution spectra were obtained with a 600 MHz DMX spectrometer and MAS NMR (^{13}C–^{13}C, ^{13}C–1H, ^{15}N–^{1}H) spectra were obtained using 600 MHz DMX and 750 MHz Bruker spectrometers. ^{13}C NMR spectra of pigments in liquid were referenced using an external standard of tetramethylsilane (TMS) with the methyl shift of 0 ppm. The ^{13}C MAS NMR of pigments in the solid state were referenced using Gly with the carbonyl chemical shift of 176.04 ppm. The ^{1}H NMR spectra of pigments in liquid were referenced using an external standard of TMS with the methyl chemical shift of 0 ppm. The ^{1}H MAS NMR spectra of pigments in solid state were referenced using TMS with the methyl chemical shift of 0 ppm. The ^{15}N NMR spectra of pigments in solution were referenced using an external standard of saturated $^{15}NH_4{}^{15}NO_3$ with a $^{15}NH_4{}^{+}$ chemical shift of 22.3 ppm towards liquid ammonia. The ^{15}N MAS NMR spectra of both pigments in solid state were referenced to solid $^{15}NH_4{}^{15}NO_3$ with a corresponding chemical shift of 23.5 ppm towards liquid ammonia.

NMR spectroscopy

^{13}C NMR in solution and in the solid state. For recording ^{13}C–^{13}C NMR spectra of the pigments in solution COSY (correlation spectroscopy) technique with the proton decoupling was used. For ^{13}C MAS RFDR NMR measurements the following acquisition parameters were applied: 90° ^{1}H pulse–4 μs, 180° ^{13}C pulse–23 μs, 90° ^{13}C pulse–12 μs, ^{13}C–^{13}C mixing time–2.5 ms, ^{13}C–^{1}H mixing time 2 ms at a ^{13}C–^{1}H Hartmann–Hahn matching condition,[29] repetition time 1 s, number of scans – 288, number of slices – 512 and number of data points in F2 dimension in one slice – 2048. Spinning frequencies of 8, 9, 10 and 13 kHz were used to assign side-bands and collect spectra of BChl *a*, and BPheo *a*. The resolution of the set of 2D spectra is sufficient to allow the identification of all 55 individual correlations and to arrive at a complete assignment of the ^{13}C response. The relatively short mixing time ensures that the observed cross-peaks in these spectra are predominantly associated with the nearest-neighbour carbon–carbon correlations.

^{1}H NMR in solution and in the solid state. For ^{1}H NMR in solution, the pulsed field gradient (PFG) heteronuclear multiple quantum coherence (HMQC) technique was used.[30] The ^{1}H NMR in solids is more difficult due to the combination of the very strong homonuclear dipolar interactions between the abundant protons and of the small chemical shift dispersion of protons. Adequate resolution can be obtained by exploiting the large ^{13}C chemical shift dispersion in ^{1}H–^{13}C Heteronuclear correlation (HETCOR) correlation spectroscopy. It has been demonstrated that high magnetic fields attenuate the ^{1}H homonuclear dipolar line broadening which is of help in ^{1}H response. In high-field MAS experiments high-spinning speeds are required to obtain sufficient resolution in the multidimensional spectra. To determine ^{1}H solid state shifts in [U–^{13}C, ^{15}N] BChl *a* and [U–^{13}C, ^{15}N] BPheo *a*, solid state CP/MAS with FSLG irradiation during the proton evolution was employed.[28] The mixing time for the CP was 0.3 ms, and the Lee–Goldberg offset was 4 or 5 kHz, with a repetition time of 1 s. For the 2D data sets the number of scans was 256, in 121 slices with 1494 data points in the F2 dimension. Since the Hartmann–Hahn matching and corresponding efficiency of CP magnetisation transfer is very sensitive to RF power instabilities at high MAS frequencies, a ramped-amplitude cross-polarisation sequence (RAMP-CP) was used to restore a broader matching profile.[31] During ^{13}C acquisition the protons were decoupled from the carbons by using a TPPM decoupling scheme. This improves the high-field ^{13}C resolution considerably compared to Continuous wave (CW) decoupling and is essential for the assignment of the heteronuclear correlation signals.[27] The phase modulation angle for the TPPM decoupling was set to 15°, and the flip-pulse length was optimised to 8.8 μs in order to yield optimal ^{13}C resolution. The magic angle pulse length was 2.44 μs. The ^{1}H shifts in the ^{1}H–^{13}C FSLG spectra of the pigments were referenced using the ^{1}H–^{13}C FSLG dataset of [U–^{13}C] Tyr as an external reference. The ^{1}H chemical shift scale was calibrated from the phase modulated LG spectrum of solid tyrosine hydrochloric salt.

^{15}N NMR in solution and in solid state. The ^{15}N NMR spectra of [U–^{13}C, ^{15}N] BChl *a* and [U–U–^{13}C, ^{15}N] BPheo *a* were referenced to an external standard, nitromethane at 380.23 ppm with respect to reference to liquid ammonia. The ^{1}H–^{15}N correlations were determined by measuring PFG heteronuclear multiple-bond

Copyright © 2008 John Wiley & Sons, Ltd.

correlation (HMBC) spectra in acetone-d_6 solution or by measuring Correlation by long-range coupling (COLOC) spectra.[16] The 1D ^{15}N CP MAS NMR spectra of pigments were recorded using the TPPM technique. The assignment of N-I and N-III in [U–^{13}C, ^{15}N] BPheo *a* was confirmed from the ^{13}C–^{15}N correlation spectrum. For obtaining ^{13}C–^{15}N MASNMR spectra a double CP pulse sequence was used.[32] CP from ^{1}H to ^{15}N was 6 μs, evolution of ^{15}N was 20 μs and CP from ^{15}N to ^{13}C was 2 ms. Data were collected in 98 slices, zero filled to 128 with 1794 data points in the F2 dimension.

Conclusion

Uniformly labelled (U–^{13}C, ^{15}N) photosynthetic pigments, BChl *a* and BPheo *a* were obtained biosynthetically and characterised with solution and solid state NMR. A complete assignment of all 55 ^{13}C solid state resonances of [U–^{13}C, ^{15}N] BChl *a* and 55 ^{13}C resonances of [U–^{13}C, ^{15}N] BPheo *a* was obtained in solution and in solid state from the analysis of 2D and ^{13}C–^{13}C COSY and CP MAS RFDR correlation spectra accordingly. The ^{1}H solution resonances of both pigments were assigned from the high-field ^{1}H–^{13}C HMQC spectra and ^{1}H solid state resonances were assigned from high-field 2D (^{1}H–^{13}C). Frequency-switched Lee–Goldburg (FSLG) dipolar correlation spectra ^{15}N solution resonances for both pigments were assigned from ^{1}H–^{15}N HMBC spectra, and ^{15}N solid state resonances of pigments were assigned from CP MAS NMR spectra. Subsequent NMR studies on a single sample allow complete assignment of ^{13}C, ^{15}N and ^{1}H resonances of the U–^{13}C, ^{15}N labelled pigments and provide details of a structure, which is considered as a fundamental basis for all follow-up ligand–protein interaction studies in photosynthesis research.

Acknowledgements

T. E. acknowledges support of the SON project of the Netherlands Organisation for scientific Research (NWO). H.J.M.d.G. is a recipient of a pioneer award of the Chemical Sciences division of the NWO. This work was partially financed by demonstration project B104-CT97-2101 of the Commission of the European communities, by a WBSO Project 2 of SenterNovem to Protein Labelling Innovation (PLI), Leiden and by PLI. Department of biophysics of LION is acknowledged for access to the HPLC facilities. Fons Lefeber is acknowledged for his assistance in NMR data processing work.

References

[1] H. J. M. de Groot, in *Biophysical Techniques in Photosynthesis*, vol. 2 (Eds: T. J. Aartsma and J. Matysik), *Series Advances in Photosynthesis and Respiration, Volume 26*, Springer: Dordrecht MAS NMR for structure determination, **2008**, pp. 361.
[2] A. G. M. Chew, D. A. Bryant, *Annu. Rev. Microbiol.* **2007**, *61*, 113.
[3] L. Limantara, P. Koehler, B. Wilhelm, R. J. Porra, H. Scheer, *Photochem. Photobiol.* **2006**, *82*, 770.
[4] P. Spolaore, C. Joannis-Cassan, E. Duran, A. Isambert, *J. Biosci. Bioeng.* **2006**, *101*, 87.
[5] R. Wijffels, *Trends Biotechnol.* **2008**, *26*, 26.
[6] S. G. Boxer, G. L. Closs, J. J. Katz, *J. Am. Chem. Soc.* **1974**, *96*, 7058.
[7] J. J. Katz, C. G. Brown, *Bull. Magn. Res.* **1983**, *5*, 3.
[8] R. J. Abraham, A. E. Rowan, in *Chlorophylls* (Ed: H. Scheer), CRC Press: **1991**, pp 797.
[9] G. Brereton, J. K. M. Sanders, *J. Chem. Soc., Perkin Trans. 1* **1983**, *1*, 435.
[10] T. Oh-hama, H. Seto, S. Miyachi, *Arch. Biochem. Biophys.* **1985**, *237*, 72.
[11] T. Oh-hama, H. Seto, S. Miyachi, *Arch. Biochem. Biophys.* **1986**, *246*, 192.
[12] J. C. Facelli, *J. Phys. Chem., B.* **1998**, *102*, 2111.
[13] R. G. Brereton., J. K. M. Sanders, *Org. Magn. Reson.* **1982**, *19*, 150.
[14] R. G. Brereton, J. K. M. Sanders, *J. Chem. Soc., Perkin Trans. 1* **1983**, *1*, 423.
[15] S. Lötjönen, T. J. Michalski, J. R. Norris, P. H. Hynninen, *Magn. Reson. Chem.* **1987**, *25*, 670.
[16] L. Limantara, Y. Kurimoto, K. Furukawa, T. Shimamura, H. Utsumi, I. Katheder, H. Scheer, Y. Koyama, *Chem. Phys. Lett.* **1995**, *236*, 71.
[17] Z.-Y. Wang, M. Umetsu, M. Kobayashi, T. Nozawa., *J. Am. Chem. Soc.* **1999**, *121*, 9363.
[18] R. J. Porra, H. Scheer, *Photosynth. Res.* **2000**, *66*, 159.
[19] Y. Kakitani, K. Harada, T. Mizoguchi, Y. Koyama, *Biochemistry* **2007**, *46*, 6513.
[20] T. A. Egorova-Zachernyuk, B. van Rossum, G.-J. Boender, E. Franken, J. Ashurst, J. Raap, P. Gast, A. Hoff, H. Oschkinat, H. J. M. de Groot, *Biochemistry* **1997**, *36*, 7513.
[21] T. A. Egorova-Zachernyuk, A. Remy, A. Ya. Shkuropatov, P. Gast, A. J. Hoff, K. Gerwert, H. J. M. de Groot, *Vib. Spectrosc.* **1999**, *19*, 347.
[22] A. J. Van Gammeren, F. B. Hulsbergen, S. Kiihne, J. G. Hollander, F. Buda, T. A. Egorova-Zachernyuk, N. Frazer, R. Cogdell, H. J. M. de Groot, *J. Am. Chem. Soc.* **2005**, *127*, 3212.
[23] H. Patzelt, B. Keûler, H. Oschkinat, D. Oesterhelt, *Phytochemistry* **1999**, *50*, 215.
[24] A. D., Egorova, L. van Wyk, H. J. J. Willems, T. A. Egorova-Zachernyuk, *5-th European Workshop on Algal Biotechnology*, **2003**, Potsdam, p P14.
[25] F. G. Acien Fernandez, J. M. Fernandez Sevilla, T. A. Egorova-Zachernyuk, E. Molina Grima, *Biomol. Eng.* **2005**, *22*, 193.
[26] T. Watanabe, K. Hongu, M. Honda, M. Nakazato, M. Korno, S. Saitoh, *Anal. Chem.* **1984**, *56*, 251.
[27] A. E. Bennet, M. Rienstra, M. Auger, K. V. Lakshmi, R. G. Griffin, *J. Chem. Phys.* **1995**, *103*, 6951.
[28] B.-J. van Rossum, H. Forster, H. J. M. de Groot, *J. Magn. Reson.* **1997**, *124*, 516.
[29] A. Pines, M. G. Gibby, J. S. Waugf, *J. Chem. Phys.* **1973**, *59*, 569.
[30] C. Griesinger, O. W. Sorensen, R. R. Ernst, *J. Magn. Reson.* **1989**, *84*, 14.
[31] G. Metz, X. Wu, S. O. Smith, *J. Magn. Reson., Ser A* **1994**, *110*, 219.
[32] M. Baldus, D. G. Geurts, S. Hediger, B. H. Meier, *J. Magn. Reson., Ser A* **1996**, *118*, 140.

 Copyright © 2008 John Wiley & Sons, Ltd.